Journal of Coordination Chemistry

ISSN: 0095-8972 (Print) 1029-0389 (Online) Journal homepage: http://www.tandfonline.com/loi/gcoo20

Syntheses, structures, and properties of two- and three-dimensional coordination polymers based on bis(imidazole) and glutarate ligands

Zhi Yang, Shan-Shan Han, Ling-Yun Zheng, Yan-Fen Peng, Bao-Long Li & Hai-Yan Li

To cite this article: Zhi Yang, Shan-Shan Han, Ling-Yun Zheng, Yan-Fen Peng, Bao-Long Li & Hai-Yan Li (2015) Syntheses, structures, and properties of two- and three-dimensional coordination polymers based on bis(imidazole) and glutarate ligands, Journal of Coordination Chemistry, 68:7, 1213-1223, DOI: 10.1080/00958972.2015.1016926

To link to this article: http://dx.doi.org/10.1080/00958972.2015.1016926

Journal of Coordination Chemistry, 2015
Vol. 68, No. 7, 1213–1223, http://dx.doi.org/10.1080/00958972.2015.1016926

Syntheses, structures, and properties of two- and three-dimensional coordination polymers based on bis(imidazole) and glutarate ligands

ZHI YANG, SHAN-SHAN HAN, LING-YUN ZHENG, YAN-FEN PENG,
BAO-LONG LI* and HAI-YAN LI

Key Laboratory of Organic Synthesis of Jiangsu Province, College of Chemistry, Chemical Engineering and Materials Science, Soochow University, Suzhou, PR China

(*Received 22 February 2014; accepted 21 January 2015*)

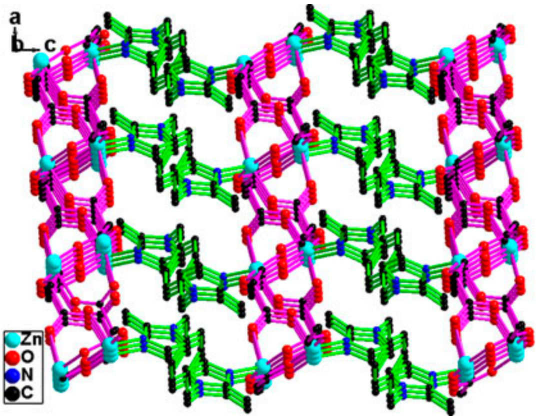

2-D and 3-D coordination polymers based on bis(imidazole) and glutarate ligands were synthesized.

Two new coordination polymers, $[Zn(bix)_{0.5}(glu)]_n$ (**1**) and $\{[Co(bix)(glu)]\cdot 4H_2O\}_n$ (**2**), were synthesized (bix = 1,4-bis(2-methylimidazol-1-ylmethyl)benzene, glu = glutarate). In **1**, each Zn(II) is connected by four glu ligands and extend to form a $[Zn(glu)]_n$ 2-D network. Adjacent $[Zn(glu)]_n$ 2-D networks are bridged by bix ligands to construct a 6-connected 3-D network based on the Zn_2 unit. **2** shows an undulated 2-D (4,4) network. The interesting structural feature of **2** is that there are 1-D water chains. The O–H···O hydrogen bond interactions link the 2-D coordination networks and construct the 3-D supramolecular architecture in **2**. The glu ligands are bis-(bidentate) bridges in **1** and bis-(monodentate) bridges in **2**. The luminescence of **1** and thermal stability of **1** and **2** were investigated.

Keywords: Zinc complex; Cobalt complex; Glutarate; 1,4-Bis(2-methylimidazol-1-ylmethyl)benzene

---

*Corresponding author. Email: libaolong@suda.edu.cn

1. Introduction

Syntheses of coordination polymers have attracted interest due to their potential applications as functional materials for luminescence, catalysis and gas absorption, and their intriguing variety of topologies [1–8]. In order to get such intriguing topologies and functional materials, the crucial step is to employ appropriate organic building blocks and metal ions. Because of the diversity of coordination modes and high structural stability, rigid aromatic polycarboxylates are frequently used for construction of coordination polymers [9, 10]. Glutarate (glu) is a flexible aliphatic ligand which can construct coordination polymers with intriguing structures but is less investigated [11–13].

Flexible bidentate N-donor ligands such as bis(imidazole) [14–19] and bis(triazole) [20–22] are widely used to construct coordination polymers due to good coordination ability. Our synthetic approach starts by focusing on the construction of new topological frameworks using flexible bis(imidazole) and bis(triazole) ligands. The flexible ligand 1,4-bis(2-methylimidazol-1-ylmethyl)benzene (bix) is a good bridging ligand for construction of coordination polymers but is not well exploited [23, 24]. The combination of the flexible glu and bix ligands can construct intriguing coordination polymers. In the present work, we synthesized two coordination polymers, $[Zn(bix)_{0.5}(glu)]_n$ (**1**) and $\{[Co(bix)(glu)]\cdot 4H_2O\}_n$ (**2**), by using bix and glutarate (glu). The structure of **1** is a 6-connected 3-D network based on the Zn_2 unit. **2** shows an undulated 2-D (4,4) network containing 1-D water chains.

2. Experimental

2.1. *Materials and general methods*

All reagents were of analytical grade and used without purification. Elemental analyses for C, H, and N were performed on a Perkin Elmer 240C analyser. IR spectra were obtained for KBr pellets on a Nicolet 170SX FT-IR spectrophotometer from 4000 to 400 cm^{-1}. Luminescence measurements were carried out in the solid-state at room temperature and the spectra were collected with a Perkin Elmer LS50B spectrofluorimeter. TGA was carried out using a Thermal Analyst 2100 TA Instrument and SDT 2960 Simultaneous TGA-DTA Instrument in flowing N_2 at a heating rate of 10 °C min^{-1}.

2.2. *Synthesis of $[Zn(bix)_{0.5}(glu)]_n$ (1)*

A solution of H_2glu (0.2 mM) in 5 mL H_2O was adjusted to pH 6.5 with 0.38 mL 1.0 M L^{-1} NaOH solution. Then bix (0.1 mM) in 5 mL CH_3CH_2OH and $Zn(NO_3)_2\cdot 6H_2O$ (0.2 mM) in 5 mL H_2O were added and stirred for 10 min. The mixture was added to a 30 mL Teflon-lined stainless steel autoclave and this was sealed and heated to 140 °C for 4 days and then cooled to room temperature. Colorless crystals of **1** were obtained in 54% yield (0.035 g). Anal. Calcd for $C_{13}H_{15}N_2O_4Zn$ (**1**) (%): C, 47.51; H, 4.60; N, 8.53. Found: C, 47.49; H, 4.57; N, 8.52. IR data (cm^{-1}): 2916w, 1628s, 1559w, 1507w, 1448w, 1414s, 1342m, 1313w, 1289w, 1267w, 1175w, 1142w, 881w, 821w, 740m, 664m, 624w.

Table 1. Crystallographic data for **1** and **2**.

	1	**2**
Formula	$C_{13}H_{15}N_2O_4Zn$	$C_{21}H_{32}CoN_4O_8$
Fw	328.64	527.44
Crystal system	Monoclinic	Monoclinic
Space group	$P2_1/a$	$P2_1/c$
Temp (K)	223(2)	223(2)
a (Å)	9.901(2)	9.666(4)
b (Å)	13.538(3)	17.712(8)
c (Å)	9.962(2)	15.214(7)
α (°)	90	90
β (°)	92.74(3)	96.820(10)
γ (°)	90	90
V (Å^3)	1333.6(5)	2586.4(19)
Z	4	4
ρ_{Calcd} (g cm^{-3})	1.637	1.354
μ (mm^{-1})	1.856	0.713
$F(0\,0\,0)$	676	1108
Reflections collected	7270	15,513
Unique reflections	3048 [R(int) = 0.0242]	5505 [R(int) = 0.0444]
Parameters	183	332
Goodness-of-fit	1.017	1.071
R_1 [$I > 2\sigma(I)$]	0.0325	0.0686
wR_2 (all data)	0.0763	0.1770

2.3. *Synthesis of {[Co(bix)(glu)]·4H$_2$O}$_n$ (2)*

A solution of H_2glu (0.2 mM) in 5 mL H_2O was adjusted to pH 6.5 with 0.38 mL 1.0 M L^{-1} NaOH solution. Then $CoCl_2\cdot 8H_2O$ (0.2 mM) in 5 mL H_2O and bix (0.2 mM) in 5 mL CH_3CH_2OH were added with continuous stirring for ten minutes at room temperature. The resulting solution was filtered. Red crystals of **2** were obtained in five days at room temperature in 43% yield (0.045 g). Anal. Calcd for $C_{21}H_{32}CoN_4O_8$ (**2**) (%): C, 47.82; H, 6.12; N, 10.62. Found: C, 47.74; H, 6.09; N, 10.58. IR data (cm^{-1}): 3395m, 3128w, 1647w, 1578s, 1543m, 1506w, 1482w, 1447m, 1416s, 1348m, 1288m, 1216w, 1141w, 1006w, 805w, 748m, 670w.

2.4. *X-ray crystallography*

Suitable single-crystals of **1** and **2** were carefully selected under an optical microscope and glued to thin glass fibers. The diffraction data were collected on Rigaku Saturn CCD diffractometers with graphite-monochromated MoK$_\alpha$ radiation. Intensities were collected by the ω scan technique. The structures were solved by direct methods and refined with full-matrix least-squares (SHELXTL-97) [25]. The non-H atoms were refined anisotropically. The positions of hydrogens of bix and glu were generated geometrically and riding on their parent atoms. The hydrogens of water were obtained from successive Fourier syntheses with constraints with O–H bond length 0.90 Å. The parameters of the crystal data collection and refinement of **1** and **2** are given in table 1. Selected bond lengths and angles are given in table 2.

Table 2. Selected bond lengths (Å) and angles (°) for **1** and **2**.

1			
Zn(1)–O(1)	2.0571(18)	Zn(1)–O(2A)	2.0198(19)
Zn(1)–O(3C)	2.0737(17)	Zn(1)–O(4B)	2.0702(17)
Zn(1)–N(2)	2.0121(19)		
O(2A)–Zn(1)–O(1)	159.27(7)	O(1)–Zn(1)–O(3C)	86.39(7)
O(1)–Zn(1)–O(4B)	88.99(8)	O(2A)–Zn(1)–O(3C)	88.92(7)
O(2A)–Zn(1)–O(4B)	88.44(8)	O(4B)–Zn(1)–O(3C)	159.66(7)
N(2)–Zn(1)–O(1)	96.04(8)	N(2)–Zn(1)–O(2A)	104.69(8)
N(2)–Zn(1)–O(3C)	102.57(7)	N(2)–Zn(1)–O(4B)	97.61(7)
2			
Co(1)–O(1)	1.957(3)	Co(1)–O(3A)	1.964(3)
Co(1)–N(2)	2.030(4)	Co(1)–N(4B)	2.019(3)
O(1)–Co(1)–O(3A)	112.52(12)	O(1)–Co(1)–N(2)	106.20(14)
O(1)–Co(1)–N(4B)	118.81(13)	O(3A)–Co(1)–N(2)	97.99(13)
O(3A)–Co(1)–N(4B)	103.91(12)	N(4B)–Co(1)–N(2)	115.55(15)

Symmetry transformations used to generate equivalent atoms: (A) $-x, -y, -z+2$; (B) $-x+1/2, y+1/2, -z+2$; (C) $x-1/2, -y-1/2, z$ for **1**; (A) $x+1, y, z$; (B) $x, -y-1/2, z-1/2$ for **2**.

3. Results and discussion

3.1. *Crystal structures*

The structure of **1** is a 6-connected 3-D network based on the Zn_2 unit. The asymmetry unit consists of one Zn(II), half bix, and one glu. Each Zn(II) displays a distorted square-pyramidal coordination geometry $\{ZnNO_4\}$, coordinated by one imidazole nitrogen from one bix (Zn(1)–N(2) 2.0121(19) Å) in the axial site, and four carboxylate oxygens from four glu ligands (Zn(1)–O(1) 2.0571(18) Å, Zn(1)–O(2A) 2.0198(19) Å, Zn(1)–O(3C) 2.0571(18) Å, Zn(1)–O(4B) 2.0702(17) Å) in the basal plane [figure 1(a)] with the structural distortion index τ 0.006 [26]. Each carboxylate of one glu is a bidentate bridge and links two Zn(II) ions. Each glu is a bis-(bidentate) bridge and joins four Zn(II) ions to form the $Zn_2(COO)_4$ unit with paddle wheel structure. The Zn–O bond lengths in **1** are 2.0198(19)–2.0702(17) Å, corresponding to the Zn–O values of $Zn_2(COO)_4$ unit with the paddle wheel structure 1.945(6)–2.015(8) Å in $[Zn(hfipbb)(H_2hfipbb)_{0.5}]_n$ [29], 2.0248 (14)–2.0711(15) Å in $[Zn_2(cbaa)_2(bpy)]_n$ [30], 2.007(2)–2.027(3) Å in $\{[Zn_4(TPOM2)(1,4\text{-}bdc)_4]\cdot DMF\cdot 4H_2O)\}_n$ [31], and 2.0398(32)–2.0442(34) Å in $[Zn_2(tbta)(DMF)_2]_n$ [32]. The Zn···Zn distance of $Zn_2(COO)_4$ unit in **1** is 2.9473(6) Å, which corresponds to the values 2.9515(5) in $[Zn_2(cbaa)_2(bpy)]_n$ [30], 2.938(2) and 2.961(3) Å in $\{[Zn_4(TPOM2)(1,4\text{-}bdc)_4]\cdot DMF\cdot 4H_2O)\}_n$ [31], and 2.9689(12) Å in $[Zn_2(tbta)(DMF)_2]_n$ [32], and is longer than 2.649(3) Å in $[Zn(hfipbb)(H_2hfipbb)_{0.5}]_n$ [29].

Each zinc(II) is connected by four glu ligands and extends to form a $[Zn(glu)]_n$ 2-D network [figures 1(b) and S1, see online supplemental material at http://dx.doi.org/10.1080/00958972.2015.1016926]. The bix ligands exhibit *anti*-conformation and bis-(monodentate) bridging. Adjacent $[Zn(glu)]_n$ 2-D networks are bridged by bix ligands with Zn···Zn distance of 14.383(2) Å to construct an unusual 3-D network $[Zn(bix)_{0.5}(glu)]_n$ with the pore of *ca.* 4 × 9 Å along the *b*-axis [figure 1(c)].

Topologically, if the Zn_2 unit is one node, then the glu is simplified as a 2-connected node. This 3-D network is simplified as a 6-connected 3-D network [figure 1(d)]. The point symbol of the 6-connected 3-D network is $(4^4 \bullet 6^{10} \bullet 8)$ [27, 28].

Some aromatic carboxylate zinc coordination polymers with paddle wheel structure are presented below for comparison with **1** because no zinc coordination polymer featuring the

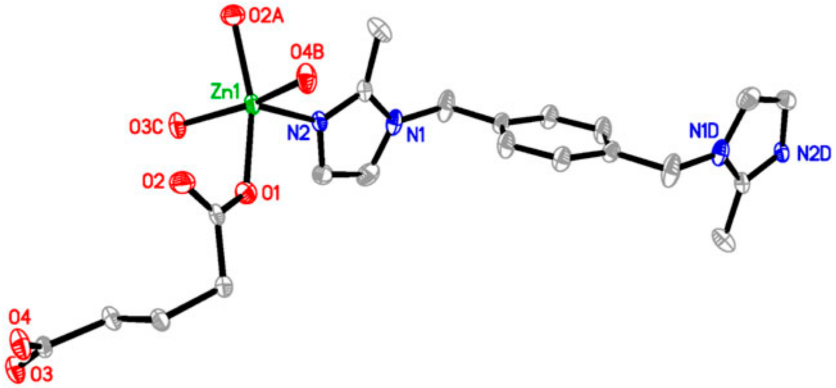

Figure 1(a). The coordination environment of the Zn(II) in **1** with 50% thermal ellipsoids.

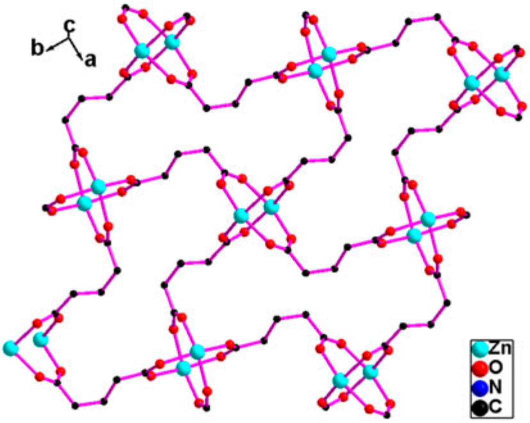

Figure 1(b). The $[Zn(glu)]_n$ 2-D network in **1**.

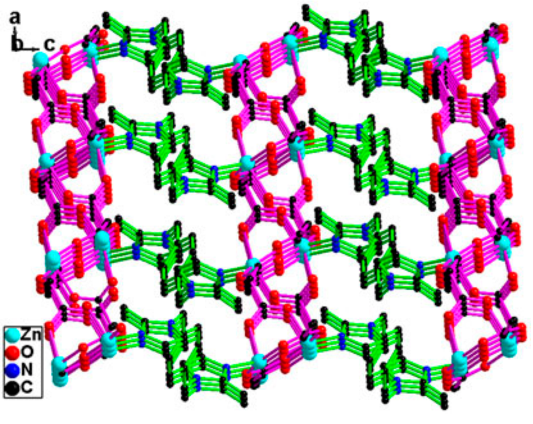

Figure 1(c). The 3-D network in **1**.

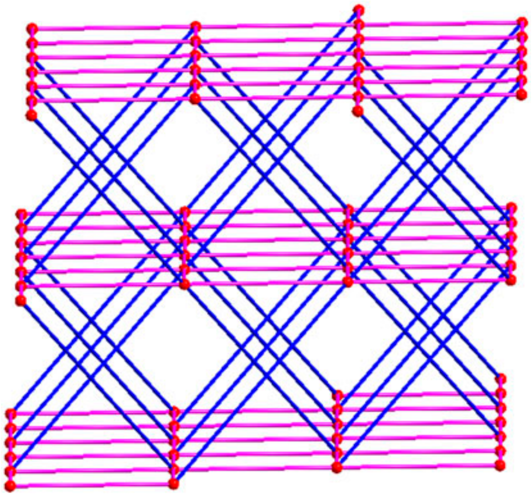

Figure 1(d). Schematic representation of the 6-connected 3-D network in **1**. The red balls are Zn_2 units. The pink and blue sticks represent the glu and bix ligands (see http://dx.doi.org/10.1080/00958972.2015.1016926 for color version).

paddle wheel structure made from aliphatic dicarboxylate was reported. $[Zn(hfipbb)(H_2hfipbb)_{0.5}]_n$ is a 3-D 2-fold interpenetrating pillared network based on paddle-wheel $[Zn_2(COO)_4]$ SUB (H_2hfipbb = 4,4′-(hexafluoroisopropylidene)bis(benzoicacid) [29]. $[Zn_2(cbaa)_2(bpy)]_n$ shows a (4,4) grid network based on $\{Zn_2(OCO)_4\}$ paddle wheel unit as the node (H_2cbaa = 4-carboxybenzeneacetic acid, bpy = 4,4′-bipyridyl) [30]. $\{[Zn_4(TPOM2)(1,4\text{-bdc})_4]\cdot DMF\cdot 4H_2O)\}_n$ exhibits a 3-D microporous coordination network constructed by typical 2-D net based on paddle wheel $[Zn_2(COO)_4]$ units and 4-connected TPOM2 ligands (TPOM2 = tetrakis(3-pyridyloxymethyl) methane, 1,4-bdc = 1,4-benzenedicarboxylate) [31]. $[Zn_2(tbta)(DMF)_2]_n$ reveals a non-catenated 3-D structure in which the framework nodes consist of Zn_2 units coordinated by carboxylates of tbta in a paddle wheel fashion (H_4tbta = 4,4′,4″,4‴-benzene-1,2,4,5-tetrayltetrabenzoic acid) [32]. $[Zn_2(sbpdc)_2(bpeb)]_n$ presents a three-folded interpenetrated 3-D framework by a typical 2-D net based on paddle wheel $[Zn_2(COO)_4]$ units and the long pillar bpeb ligands (H_2sbpdc = sulfone-4,4′-biphenyldicarboxylic acid, bpeb = 1,4-bis(4-pyridylethynyl) benzene). The structure of $\{[Zn_2(sbpdc)_2(bpy)]\cdot 4DMF\}_n$ is similar to that of $[Zn_2(sbpdc)_2(bpeb)]_n$, but is a two-folded interpenetrated framework due to the presence of a shorter pillar bpy ligand (bpy of *ca.* 7 Å) which is less than half of bpeb (*ca.* 16 Å) [33].

2 shows an undulated 2-D (4,4) network containing 1-D water chains. The asymmetric unit consists of one cobalt(II), one bix, one glu, and four lattice waters. Each Co(II) displays a distorted tetrahedral coordination geometry $\{CoN_2O_2\}$, coordinated by two imidazole nitrogens from two bix ligands, and two carboxylate oxygens from two glu ligands [figure 2(a)]. The Co–N bond lengths are 2.030(4) and 2.019(3) Å and the Co–O bond lengths are 1.957(3) and 1.964(3) Å, which are in the normal range for distorted tetrahedral Co(II) coordination complexes. For example, the Co–N bond lengths are 2.009(4) and 2.010(3) Å for $\{[Co(bpdc)(bimb)](DMF)_3\}_n$ (H_2bpdc = biphenyl-4,4′-dicarboxylic acid, bimb = 1,4-bis(imidazol-l-ylmethyl)benzene) [34], 2.032(3) Å for $[Co(bmimb)_{0.5}(hip)]_n$ (bmimb = 1,4-bis(5,6-dimethylbenzimidazole)butane, H_2hi*p* = 5-hydroxyisophthalic acid)

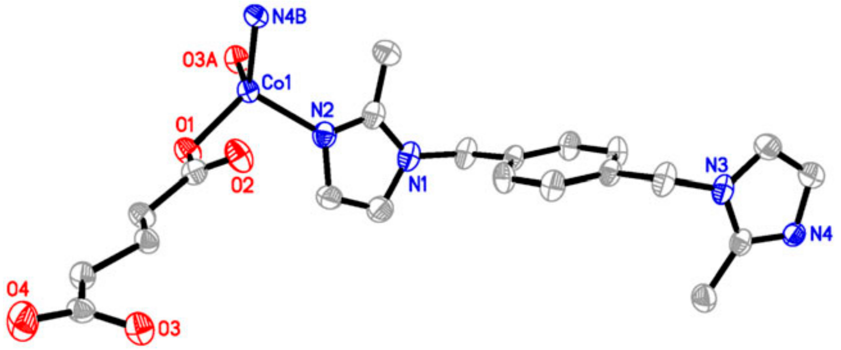

Figure 2(a). The coordination environment of the Co(II) in **2** with 50% thermal ellipsoids.

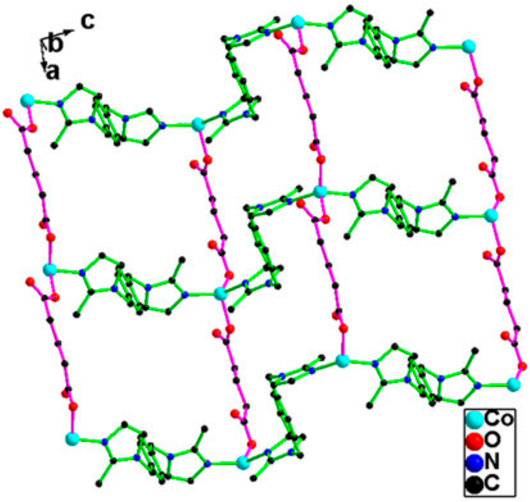

Figure 2(b). The undulated 2-D network in **2**.

[35], 1.999(3) Å for $[Co(mimba)(H_2O)]_n$ (H_2mimba = 5-((2-methyl-1H-imidazol-1-yl) methyl)benzene-1,3-dioic acid) [36], 2.009(3) and 2.024(3) Å for $\{[Co_2(mdip)(m\text{-}bix)_2]2H_2O\}_n$ (H_4mdip = methylenediisophthalic acid, m-bix = 1,3-bis(imidazole-1-ylmethyl)benzene) [37]. The Co–O bond lengths are 1.946(3) and 1.963(3) Å for $\{[Co(bpdc)(bimb)](DMF)_3\}_n$ [34], 1.958(4) and 1.965(3) Å for $[Co(bmimb)_{0.5}(hip)]_n$ [35], 1.947(2) and 2.021 (2) Å for $[Co(mimba)(H_2O)]_n$ [36], 1.958(2) and 1.990(3) Å for $\{[Co_2(mdip)(m\text{-}bix)_2]2H_2O\}_n$ [37]. The Co–O distances for Co1–O2 and Co1–O4A are 2.733(2) and 3.062(2) Å, showing the weak interactions.

The bix ligands exhibit the *anti*-conformation and bis-monodentate bridging mode. The glu ligands are bis-(monodentate) bridging. Each node (Co(II)) is surrounded by four nodes (Co(II) ions) which are bridged by bix and glu ligands [figure 2(b)]. Four Co(II) ions, two bix and two glu ligands form a $[Co_4(bix)_2(glu)_2]$ unit with the Co···Co distances 14.261(5) and 9.666(4) Å for bix and glu bridges.

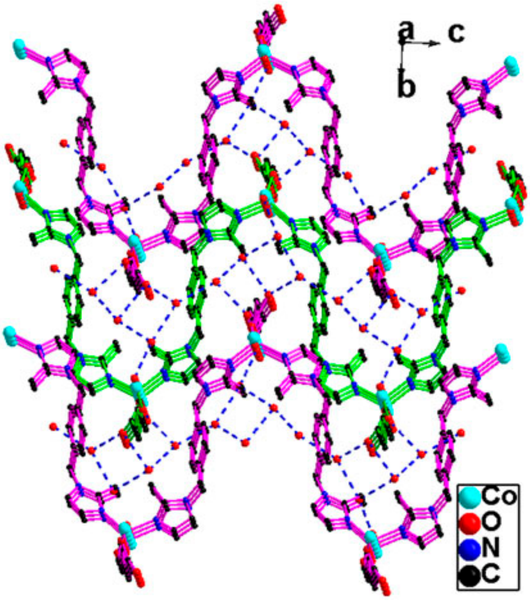

Figure 2(c). The 3-D supramolecular architecture in **2**. The blue dashed lines exhibit the O–H···O hydrogen bond interactions (see http://dx.doi.org/10.1080/00958972.2015.1016926 for color version).

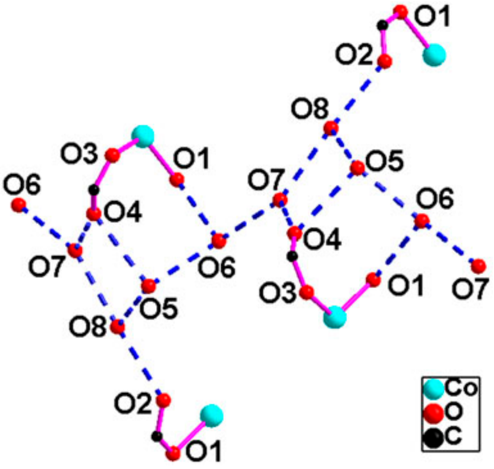

Figure 2(d). The 1-D water chain in **2**. The blue dashed lines exhibit the O–H···O hydrogen bond interactions (see http://dx.doi.org/10.1080/00958972.2015.1016926 for color version).

The parallel 2-D networks stack along the *a*-axis. The shortest Co···Co distance between two adjacent 2-D networks is 9.666(4) Å [figures 2(c) and S2]. The interesting structural feature of **2** is that there are 1-D water chains [38, 39]. The O–H···O hydrogen bond interactions between the lattice water molecules (O5, O6, O7, O8) result in the 1-D water chains [figure 2(d), table 3]. The distances of O5···O6, O6···O7, O7···O8, and O8···O5 are 2.728 (7), 2.777(7), 2.889(8), and 2.833(7) Å, respectively. The O–H···O hydrogen bond

Table 3. Hydrogen bonding for **2** (Å and °).

D–H···A	*d*(D–H)	*d*(H···A)	D(D···A)	∠(DHA)
O(5)–H(1W)···O(6)	0.93(2)	1.91(4)	2.728(7)	145(6)
O(5)–H(2W)···O(4)$^{\text{i}}$	0.904(19)	2.07(2)	2.960(6)	166(5)
O(6)–H(3W)···O(1)	0.91(2)	1.90(2)	2.799(5)	173(7)
O(6)–H(4W)···O(7)$^{\text{ii}}$	0.92(2)	1.91(3)	2.777(7)	156(6)
O(7)–H(5W)···O(8)	0.91(2)	2.06(5)	2.889(8)	150(8)
O(7)–H(6W)···O(4)$^{\text{i}}$	0.90(2)	2.01(6)	2.751(6)	138(8)
O(8)–H(7W)···O(2)$^{\text{iii}}$	0.90(2)	2.01(3)	2.870(6)	181(7)
O(8)–H(8W)···O(5)	0.897(19)	1.96(3)	2.833(7)	166(8)

Symmetry transformations used to generate equivalent atoms: (i) $x+1, y, z$; (ii) $x, -y-3/2, z+1/2$; (iii) $-x, y-1/2, -z+1/2$.

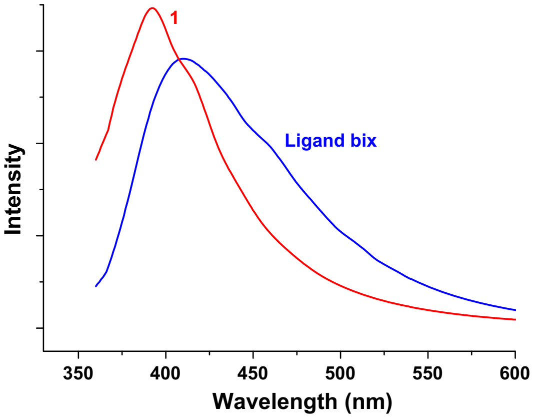

Figure 3. The solid-state emissions of **1** and free bix ligand at room temperature.

interactions between lattice water and carboxylate oxygens of glu ligands sustain the water chains. The hydrogen bond interactions link the 2-D coordination networks and construct the 3-D supramolecular architecture [figure 2(c)].

Some Co(II) coordination polymers with distorted tetrahedral geometry are cited for comparison because the Co(II) ion is four-coordinate in a distorted tetrahedral geometry in **2**. $\{[Co(bpdc)(bimb)](DMF)_3\}_n$ exhibits a (6,3) layer consisting of hexagonal meshes and loops [34]. $[Co(bmimb)_{0.5}(hip)]_n$ presents a 2-D (4,4) network [35]. $[Co(mimba)(H_2O)]_n$ shows a two-fold interpenetration 3-D framework [36]. $\{[Co_2(mdip)(m\text{-}bix)_2]2H_2O\}_n$ exhibits an interesting unsquare 2-D (4,4)-connected net with helical character [37].

3.2. *PXRD and photoluminescent properties*

The measured and simulated PXRDs confirm the purity of **1** and **2** (figures S3 and S4). The d^{10} metal compounds exhibit some interesting photoluminescence properties. The solid-state luminescence spectra of **1** and free bix at room temperature are given in figure 3. The free bix ligand in the solid-state shows the emission band maximum at 409 nm upon excitation at 340 nm. **1** exhibits the strong emission band maximum at 392 nm upon excitation at 340 nm. **1** shows the blue-shift of emission by 17 nm when compared to free bix. The

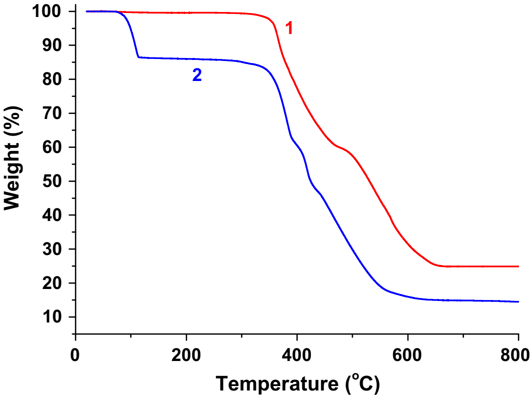

Figure 4. The TG curves of **1** and **2**.

emission of **1** can be tentatively attributed to a mixture of characteristics of intraligand and ligand-to-ligand charge transfer (LLCT) [40, 41].

3.3. *Thermal analysis*

To characterize the thermal stability, the thermal behaviors of **1** and **2** were examined by TGA. The experiments were performed on samples consisting of numerous single-crystals with a heating rate of 10 °C min^{-1} (figure 4). Compound **1** is stable to 325 °C. Then weight loss continuously occurred until 670 °C. The residue should be ZnO (Calcd: 24.77%, found: 24.86%). For **2**, the lattice waters were lost from 50 to 118 °C (Calcd: 13.66%, found: 13.58%). The anhydrous matter is thermally stable upon heating to 290 °C. Then weight loss continuously occurred until 650 °C. The residue may be CoO (Calcd: 14.21%, found: 14.47%).

4. Conclusion

Two new coordination polymers, $[\text{Zn(bix)}_{0.5}\text{(glu)}]_n$ (**1**) and $\{[\text{Co(bix)(glu)}]\cdot 4\text{H}_2\text{O}\}_n$ (**2**), were synthesized (bix = 1,4-bis(2-methylimidazol-1-ylmethyl)benzene, glu = glutarate). The structure of **1** is a 6-connected 3-D network based on the Zn_2 unit. **2** shows an undulated 2-D (4,4) network containing 1-D water chains. The glu ligands are bis-(bidentate) bridges in **1** and bis-monodentate bridges in **2**. The different structures of **1** and **2** may be attributed to different coordination geometry of metal centers and different coordination modes of glu ligands. Combination of N-heterocyclic and polycarboxylate ligands is a good choice for construction of coordination polymers with specific structures and properties.

Supplementary material

Crystallographic data for the structural analysis have been deposited with the Cambridge Crystallographic Data Center with CCDC numbers 987951 and 987952.

Funding

This work was supported by the National Natural Science Foundation of China [grant number 21171126]; the Priority Academic Program Development of Jiangsu Higher Education Institutions; the Funds of Key Laboratory of Organic Synthesis of Jiangsu Province.

References

[1] S.R. Batten, R. Robson. *Angew. Chem. Int. Ed.*, **37**, 1460 (1998).
[2] Z. Su, M. Chen, T. Okamura, M.S. Chen, S.S. Chen, W.Y. Sun. *Inorg. Chem.*, **50**, 985 (2011).
[3] D. Banerjee, S.J. Kim, H. Wu, W. Xu, L.A. Borkowski, J. Li, J.B. Parise. *Inorg. Chem.*, **50**, 208 (2011).
[4] T. Ni, M. Shao, S. Zhu, Y. Zhao, F. Xing, M.X. Li. *Cryst. Growth Des.*, **10**, 943 (2010).
[5] J.P. Zhang, Y.B. Zhang, J.B. Lin, X.M. Chen. *Chem. Rev.*, **112**, 1001 (2012).
[6] T.R. Cook, Y.R. Zheng, P.J. Stang. *Chem. Rev.*, **113**, 734 (2013).
[7] H.P. Wang, H.L. Wang, H.Y. Li, B.L. Li. *J. Coord. Chem.*, **65**, 1803 (2012).
[8] S. Zhao, Y. Yang, Z. Yang, B.L. Li, Y. Zhang. *J. Coord. Chem.*, **66**, 789 (2013).
[9] F.X. Yue, X.Y. Yu, Y.H. Luo, J.J. Yang, X. Chen, H. Zhang. *J. Coord. Chem.*, **66**, 2843 (2013).
[10] C. Yang, F.P. Huang, H.Y. Li, D. Yao, H.D. Bian. *J. Coord. Chem.*, **66**, 3939 (2013).
[11] X.X. Xu, Y. Ma, Y. Lu, E.B. Wang, X.L. Bai. *J. Coord. Chem.*, **60**, 547 (2007).
[12] X.X. Xu, Y. Ma, Y. Lu, E.B. Wang. *J. Coord. Chem.*, **60**, 1005 (2007).
[13] D.Y. Wei, H.Z. Xie, S.J. Huang, J. Zhou, G.X. Lu. *J. Coord. Chem.*, **64**, 424 (2011).
[14] X. Zhu, J.W. Zhao, B.L. Li, Y. Song, Y.M. Zhang, Y. Zhang. *Inorg. Chem.*, **49**, 1266 (2010).
[15] Z.M. Man, F. Guo. *J. Coord. Chem.*, **66**, 1 (2013).
[16] J.H. Zhou, Y. Wang, S.N. Wang, T. Wang, Y.C. Chen, G.X. Liu. *J. Coord. Chem.*, **66**, 737 (2013).
[17] B.F. Huang, H.P. Xiao, H. Huang, X.H. Li, J.G. Wang, A. Morsali. *J. Coord. Chem.*, **66**, 904 (2013).
[18] X.Y. Hou, X. Wang, F. Fu, J.J. Wang, L. Tang. *J. Coord. Chem.*, **66**, 3126 (2013).
[19] Z. Sun, Y.S. Ding, L.J. Tian, X.T. Zhang. *J. Coord. Chem.*, **66**, 763 (2013).
[20] G. Aromí, L.A. Barrios, O. Roubeau, P. Gamez. *Coord. Chem. Rev.*, **255**, 485 (2011).
[21] M.L. Han, J.G. Wang, L.F. Ma, H. Guo, L.Y. Wang. *CrystEngComm*, **14**, 2691 (2012).
[22] H.P. Wang, X.G. Liu, X. Zhu, B.L. Li, B. Wu. *J. Coord. Chem.*, **64**, 4254 (2011).
[23] L. Dobrzańska, G.O. Lloyd, H.G. Raubenheimer, L.J. Barbour. *J. Am. Chem. Soc.*, **127**, 13134 (2005).
[24] L. Dobrzańska, H.G. Raubenheimer, L.J. Barbour. *Chem. Commun.*, 5050 (2005).
[25] G.M. Sheldrick. *Acta Crystallogr.*, **64**, 112 (2008).
[26] A.W. Addison, T.N. Rao, J. Reedijk, J. van Rijn, G.C. Verschoor. *J. Chem. Soc., Dalton Trans.*, 1349 (1984).
[27] V.A. Blatov, M. O'Keeffe, D.M. Proserpio. *CrystEngComm*, **12**, 44 (2010).
[28] E.V. Alexandrov, V.A. Blatov, A.V. Kochetkov, D.M. Proserpio. *CrystEngComm*, **13**, 3947 (2011).
[29] Y.P. Wu, D.S. Li, F. Fu, W.W. Dong, J. Zhao, K. Zou, Y.Y. Wang. *Cryst. Growth Des.*, **11**, 3850 (2011).
[30] G.Z. Liu, X.D. Li, L.Y. Xin, X.L. Li, L.Y. Wang. *J. Solid State Chem.*, **203**, 106 (2013).
[31] F. Yu, W.J. Yu, B. Li, T.L. Zhang. *CrystEngComm*, **14**, 6770 (2012).
[32] O.K. Farha, K.L. Mulfort, J.T. Hupp. *Inorg. Chem.*, **47**, 10223 (2008).
[33] T. Yamada, S. Iwakiri, T. Hara, K. Kanaizuka, M. Kurmoo, H. Kitagawa. *Cryst. Growth Des.*, **11**, 1798 (2011).
[34] X.Z. Song, S.Y. Song, C. Qin, S.Q. Su, S.N. Zhao, M. Zhu, Z.M. Hao, H.J. Zhang. *Cryst. Growth Des.*, **12**, 253 (2012).
[35] L. Qin, J. Zheng, S.L. Xiao, X.H. Zheng, G.H. Cui. *Inorg. Chem. Commun.*, **34**, 71 (2013).
[36] R.W. Huang, B. Li, Y.Q. Zhang, Y. Zhao, S.Q. Zang, H. Xu. *Inorg. Chem. Commun.*, **39**, 106 (2014).
[37] X.Y. Duan, J.H. Zhao, M.L. Wei. *J. Mol. Struct.*, **1056–1057**, 333 (2014).
[38] Y.N. Gong, C.B. Liu, X.H. Tang, A.Q. Zhang. *J. Coord. Chem.*, **64**, 2761 (2011).
[39] L.J. Yuan, G.X. Huang, S.P. Chen, Z. Peng. *J. Coord. Chem.*, **61**, 3575 (2008).
[40] P. Du, Y. Yang, J. Yang, Y.Y. Liu, W.Q. Kan, J.F. Ma. *CrystEngComm*, **15**, 6986 (2013).
[41] S. Sengupta, S. Ganguly, A. Goswami, P.K. Sukul, R. Mondal. *CrystEngComm*, **15**, 8353 (2013).